Hybrid synthesis of AMFC-derived amides using supported gold nanoparticles and acyl-coenzyme A ligases

Lucas Bisel,[a]‡ Aurélie Fossey-Jouenne,[b]‡ Richard Martin,[a]‡ Jonathan Bassut,[a]‡ Antoine Lancien,[c] Louis Mouterde,[d] Vivien Herrscher,[d] Muriel Billamboz,[e] Carine Vergne-Vaxelaire,[b] Rénato Froidevaux,[c] Anne Zaparucha,*[b] and Egon Heuson*[a]

By integrating different types of catalysts in the same system, hybrid catalysis emerges as an attractive and competitive approach. Within the framework of valorizing sustainably sourced bio-based products, we herein present a synthetic method for producing amides from alcohols and the bio-sourced *5*-aminomethyl-*2*-furancarboxylic acid (AMFC). This approach utilizes supported gold metal nanoparticles as heterogeneous chemocatalysts, in conjunction with an acyl-coenzyme A ligase (ACL). By combining the actions of these catalysts, aliphatic mono- and di-alcohols are converted to the corresponding AMFC-derived amides with yields of up to 65% in aqueous buffer at 60 °C. This process requires only the addition of the enzyme and associated reactants in the same vessel for the second step in an one-pot/two-steps procedure.

Introduction

The 9th principle of green chemistry states: "catalytic reagents (as selective as possible) are superior to stoichiometric reagents".[1] Catalysis is nowadays a widely implemented approach to improve the atom economy and reduce the energy required for certain chemical transformations, which are sometimes impossible without the employment of a catalyst. In this context, hybrid chemoenzymatic catalysis emerges as an outstanding strategy that takes advantage of the two different and sometimes antagonistic fields in catalysis: heterogeneous catalysis and biocatalysis.[2–4] This combination can provide effective catalytic routes for processes which still need improvements to become part of a sustainable economy.

Amide synthesis is one of the most important transformations in agrochemicals, pharmaceuticals and polymer industries.[5–7] In recent decades, there has been growing interest in processes for obtaining amides after the ACS Green Chemistry Institute pointed out the need for more sustainable approaches for amide production as a key research area for a more environmentally friendly chemistry.[8] The most common approach for producing amides is the nucleophilic addition of an amine to an activated carboxylic acid. However, the activating agents involved in these reactions often lead to the generation of waste and hazardous byproducts.[9,10]

Alternatively, biocatalysis is currently seen as a powerful tool for the sustainable synthesis of a wide range of compounds. Enzymes, owing to their biological roles, exhibit high chemo-, regio-, and often stereoselectivity. Additionally, enzymatic reactions typically occur in aqueous medium under mild conditions. Industrially, amides have been synthesized using mainly hydrolases (such as lipases, esterases, and acylases), nitriles hydratases, and transglutaminases.[11] In addition, the repertoire of enzymes known to catalyze the amide bond formation includes thioesterases (TEs) from both polyketide synthase (PKS) and non-ribosomal peptide synthetases (NRPS) systems, stand-alone adenylation domains (SAADs), carboxylic acid reductases (CARs), amide-bond synthetases (ABSs), AMP-ligating enzymes and acyl-coenzyme A ligases (ACLs).[11–20]

ACLs are enzymes belonging to the adenylate-forming enzyme superfamily, which comprises acyl- and aryl CoA synthetases, non-ribosomal peptide synthetases, and luciferases, being responsible for a variety of biological processes. ACLs catalyze ATP-dependent formation of acyl-CoA thioesters from carboxylic acids in two-step reaction: first formation of adenylate derivative from carboxylic acid and ATP, second, nucleophilic attack of coenzyme A (HSCoA).[21] Diversion of the native reaction by adding extra amine nucleophile in absence of HSCoA leads to the formation of amides.[20,22–24] Thus, ACLs represent an alternative biocatalytic system for amide synthesis. Combined with upstream catalytic formation of carboxylic acids from alcohols available from renewable sources, this process offers a sustainable pathway for amide synthesis. This strategy, with sequential catalytic steps where each step is catalyzed by a different type of catalyst, here heterogeneous catalyst and biocatalyst, is called hybrid catalysis. It has the advantage of concentrating all the reagents and catalysts in one and the same reaction medium, which limits energy consumption, eliminates intermediate purification, and therefore the cost in atoms, and makes it possible to carry out the synthesis of compounds that were previously difficult to access.[2–4,25–28] In particular, several studies have already demonstrated the interest of coupling gold nanoparticles with different families of enzymes for the construction of innovative reaction cascades, in particular in order to introduce chirality into new building blocks.[29–33]

We have recently exemplified the capacity of hybrid catalysis through the production of a new non-natural aromatic ω-amino acid, resulting from the oxidation and successive amination of *5*-hydroxymethylfurfural (HMF): the *5*-aminomethyl-*2*-

[a] Univ. Lille, CNRS, Centrale Lille, Univ. Artois, UMR 8181-UCCS-Unité de Catalyse et Chimie du Solide, F-59000 Lille, France
[b] Génomique Métabolique, Genoscope, Institut François Jacob, CEA, CNRS, Univ Evry, Université Paris-Saclay, Evry, France
[c] UMR Transfrontalière BioEcoAgro N◦ 1158, Univ. Lille, INRAE, Univ. Liège, UPJV, JUNIA, Univ. Artois, Univ. Littoral Côte d'Opale, Institut Charles Viollette,59655 Villeneuve d'Ascq, France
[d] URD Agro-Biotechnologies Industrielles (ABI), CEBB, AgroParisTech Innovation, Pomacle, France
[e] ICL, JUNIA, Université Catholique de Lille, LITL, F-59000 Lille, France.
‡ These authors contributed equally to this work.

furancarboxylic acid (AMFC).[34] In addition to being a potential monomer for polymerization into new polyamides,[35] it serves as a valuable and versatile platform molecule due to its acid and amine functions. To date, no functionalization of AMFC has yet been achieved. Grafting variable-length aliphatic chains onto one of these functions could lead to the formation of amphiphilic molecules. In such a structure, the remaining ionisable function would act as the polar head, while the aromatic ring and the long chain constitute the apolar part. In a first approach, we planned to use the amine function as anchoring point for long chain amides. To achieve this, we combined the oxidation of various alcohols into carboxylic acids using a heterogeneous chemocatalyst with the formation of amides, employing AMFC as the amine donor and catalyzed by an ACL enzyme. This approach enables us to introduce a novel hybrid system for the direct synthesis of long chain amides from AMFC and aliphatic alcohols (Scheme 1).

Scheme 1

To demonstrate the feasibility of this approach, we initially focused on identifying suitable catalysts. ACL was selected after screening eight enzymes, sourced from prior studies, against carboxylic acids of various chain lengths. The chemocatalyst for alcohol oxidation was chosen based on previous results. After confirming its compatibility with the enzymatic reaction conditions, we evaluated the potential to combine the two catalytic processes sequentially in a one-pot/two-steps procedure. This approach enabled the synthesis of five AMFC-based amides: four with aliphatic chains from C4 to C8, and one as a diamide product from succinic acid. This represents the first proof of concept and paves the way for developing a hybrid one-pot/one-step process. The results reported here serve as a foundation for further development in the synthesis of AMFC-based derivatives and the advancement of hybrid processes involving these two families of catalysts.

Results and discussion

Screening of ACLs

In a first step, eight ACLs were screened for activity towards 12 aliphatic-, phenyl substituted-, mono- and di-carboxylic acids (**1b-12b**, Figure 1). These thermophilic enzymes were selected based on previous results (Table S1).[13] The screening was conducted in the presence of slight excess of AMFC as nucleophilic amine in MOPS buffer at pH 8 at the temperature of 60 °C to promote the spontaneous nucleophilic aminolyse of the adenylate intermediate (Scheme 2).

Scheme 2
Figure 1

In our work on ACLs, we observed that these enzymes generally exhibit stability and tolerance across a wide range of buffers and pH levels, with optimal activity around pH 8. Both Mn and Mg cations were added to ensure the optimum activity of the enzymes under the screening reaction conditions, as we have previously observed that ACLs can have a preference for one or the other of the cations. From the 12 mono and dicarboxylic acids, 11 were found to be substrates of at least one ACL, although only traces of the corresponding amide were formed when dicarboxylic malonic (**10b**) and succinic acids (**11b**) were used (Figure 2). None of the selected enzymes was active towards fumaric acid (**12b**). As expected, AMFC proved to be as sufficiently good nucleophile to allow amide formation via non-catalyzed addition to the adenylate intermediate. All the selected ACLs demonstrated activity towards most of the substrates. Among the eight enzymes, four exhibited distinct profiles: as already observed, *Ms*ACL demonstrated a preference for short aliphatic carboxylic acids, while *Ch*ACL showed activity mostly towards long aliphatic carboxylic acids.[20,36,37] *Gt*ACL displayed a broad substrate range, being active towards all the tested monocarboxylic acids, although it yielded low result with aromatic substrate **7b**. The most promiscuous enzyme, *Ts*ACL, facilitated the conversion of all three types of substrates: short- to long-chain monocarboxylic acids, monocarboxylic acids with a phenyl moiety, and succinate, a dicarboxylic acid. Analytical yields were determined by coupled enzymatic assay (Scheme S1), giving moderate to excellent results (Figure 2, Table S2).

Figure 2

In parallel, it was assessed whether AMFC could also be substrate for ACLs, through its carboxylic acid function, by carrying out reactions in the presence of butylamine as an external nucleophile on one side, and without any nucleophile on the other one, to assess AMFC's ability to react on itself and form dimer. This evaluation was carried out on a representative subset of enzymes (*Ms*ACL, *Ts*ACL and *Gt*ACL). AMFC proved to be a poor substrate for the selected ACLs, producing only traces of the corresponding butylamide in the presence of butylamine. Furthermore, in the absence of an external nucleophile, the reaction failed to produce any dimer (data not shown).
Among the enzymes with promising profiles, we chose to focus on *Ts*ACL due to its higher substrate promiscuity and its ability to convert carboxylic acids with good yields under the tested reaction conditions.

Heterogeneous catalyst: study under the reaction conditions of the enzymatic step

For efficient tandem catalysis, both catalysts – in this case, nanoparticles and the enzyme – must operate effectively under similar conditions. Based on a previous study, we selected our recently developed Au/CaO catalyst due to its demonstrated ability to oxidize a wide range of aliphatic alcohols into the corresponding carboxylic acids with yields exceeding 95 % within 24 h (10 mM scale) in several enzyme-compatible buffers, including the MOPS, which was used for the ACL screening. However, the compatibility of this catalyst with ACL operating conditions, particularly its ability to function in the presence of the cofactors such as Mg or Mn, had not yet been fully established. Therefore, we investigated the influence of buffer type and pH on the activity of the Au/CaO catalyst in the

presence of 5 mM cofactor at 60 °C. Although if we previously observed complete inhibition of the catalyst in TRIS-HCl, we decided to retain this buffer in the study because the metal cofactor might provide a protective effect. We varied the pH of each buffer according to its capacity, to resolve a range from 8 to 11 (MOPS pH 8-9, TRIS-HCl pH 9-10, CAPS pH 10-11). It should be noted that the screening of different buffers was carried out only with the addition of Mg, at the exception of MOPS pH 8, which was also tested in the presence of 5 mM Mn and a Mg/Mn mixture, both at a concentration of 5 mM, to test the influence of the nature of the metal cation. Finally, butanol (**1a**) was chosen as model substrate for this screening thank to its high solubility in buffers. The results are shown in Table 1.

Table 1

The best results were obtained in the presence of MOPS with 5 mM $MgCl_2$. Consistent with our previous observations regarding gold nanoparticle activity, we achieved substantially better conversion at pH 9 compared to pH 8, with butyric acid (**1b**) yields of 84 % and 79 % respectively, after 24 h at 60 °C (Figures S6-8). This aligns with the fact that this type of catalyst performs best at more basic pH levels. At higher pH levels, using TRIS-HCl and CAPS buffers, the results were less satisfactory, with no butyric acid (**1b**) formation in TRIS, and yields of 36 % and 56 % for CAPS at pH 10 and pH 11 respectively (Figures S9-16). This demonstrates the negative influence of these two buffers, especially TRIS, which completely inhibits the activity of gold nanoparticles as previously observed. In CAPS buffer, we still observed a positive effect of increasing pH, although the yields are lower compared to those obtained in MOPS buffer. Despite the best yield appearing slightly lower compared to the conversion observed in our previous study using the same buffer without Mg, we were able to achieve a 94 % yield in 24 h by replicating these same conditions with a freshly prepared Au/CaO (Table 2, Figure S17). This shows that the presence of Mg cation has little or no effect on catalyst activity, and that the catalyst is sensitive and requires careful storage conditions. Consequently, all subsequent experiments were carried out with freshly prepared catalyst. Regarding the influence of the metal cation, we observed a decrease in yield at 24 h in the presence of $MnCl_2$, with 48 % and 50 % of butyric acid (**1b**) formed in the presence of 5 mM of $MgCl_2$, and a combination of 5 mM of both $MnCl_2$ and $MgCl_2$ respectively, compared to 79 % when only $MgCl_2$ was added (Figures S18-19). This suggests that the manganese ion inhibits partially the activity of the gold nanoparticles, although the exact mechanism remains unknown. The nature of the metal cation thus appears to be a critical parameter for the implementation of tandem catalysis. Finally, we also observed a noticeable degradation of CAPS and MOPS buffers, with their concentrations decreasing during the reaction according to HPLC monitoring, coupled to the appearance of new, unknown peaks. For TRIS-HCl buffer this effect was much less pronounced.

Overall, our findings revealed that the reaction conditions of the enzymatic reaction, i.d. MOPS buffer pH 8 at 60 °C, are suitable for the oxidation step catalyzed by gold nanoparticles. The Mg cation was retained as its presence as a negligible effect on carboxylic acid yield, which is not the case with Mn cation. Even if the yield in carboxylic acid was higher at pH 9 than at pH 8, the difference was not significant, with very high yields within 24 h in both cases.

We then investigated the formation of carboxylic acids from various alcohols through oxidation catalyzed by gold nanoparticles under the same reaction conditions as the enzymatic step. In addition to using butanol (**1a**) as model substrate, we conducted reactions with pentanol (**2a**), hexanol (**3a**), octanol (**5a**), *2*-phenylethanol (**7a**) and *1*,*4*-butandiol (**11a**)(Figure S3). These alcohols were chosen because their corresponding carboxylic acids are substrates of *Ts*ACL, the selected enzyme. Consistent with our previous study, we achieved excellent conversion into the corresponding acids for all the aliphatic alcohols tested (91 % for **2b**, 93 % for **3b**, 88 % for **5b** and > 95 % for **11b**) as reported in Table 2 (Figures S21-24). In contrast, we did not measure any conversion for the *2*-phenylethanol. Noteworthy, in the case of *1*,*4*-butanediol, total oxidation of both carboxylic acids was observed showing the efficacy of our catalyst, and making it promising to produce dimers of AMFC-amides.

Table 2

One-pot/two-steps catalytic process

The final objective was to combine the metal-catalyzed oxidation of alcohols with the biocatalyzed amidation in a one-pot/two-steps process. More specifically, the process consisted in carrying out the oxidation step under the enzymatic reaction conditions (MOPS buffer, $MgCl_2$, 60 °C), then to add ATP, AMFC and the enzyme, without modification of the operating conditions, in the manner of a fed-batch. For the first step, Au/CaO was used at a concentration of 0.8 % (w/v) (8 mg in 1 mL). With a 2 % (w/w) Au loading, and 10 mM alcohol substrate, this represents a substrate/active phase concentration ratio of 12, without any optimization yet performed. The tandem process was first investigated with model substrate butanol (**1a**) leading to the formation of *5*-(butyramidomethyl)furan-*2*-carboxylic acid (**1c**). Butanol oxidation by Au/CaO was performed at 60 °C in MOPS buffer pH 8 with 5 mM $MgCl_2$, on an axial rotary agitator to ensure optimal mixing of the heterogeneous reaction medium. The product formation was monitored by ^{1}H NMR and, as expected, 94% yield was obtained in 24 h (Table 3, Figure S25-26). Then, *Ts*ACL, AMFC, and ATP were added, along with some $MgCl_2$ to maintain its concentration at 5 mM despite dilution, and the reaction mixture was placed at 60 °C for an extra 24 h. A final yield of 65 % in *5*-(butyramidomethyl)furan-*2*-carboxylic acid (**1c**) was achieved according to ^{1}H NMR monitoring, which is very similar to the 71 % yield obtained during ACL screening with this enzyme and butanoic acid (**1b**). This initial reaction demonstrates the feasibility of coupling the two steps. Importantly, the presence of the chemical catalyst does not significantly inhibit the enzyme.

Table 3
Figure 4

The synthetic potential of the tandem process was further explored with pentanol (**2a**), hexanol (**3a**), octanol (**5a**), and *1,4*-butandiol (**11a**), the previously tested alcohols. No attempt was made with *2*-phenylethanol (**7a**) as it was not converted by the Au/CaO. Very high conversion of all the alcohols into the corresponding carboxylic acids was observed after 24 h as expected from previous results (Table 3, Figures S27-32). Interestingly, *5*-(pentanamidomethyl)furan-*2*-carboxylic acid (**2c**) and *5*-(hexanamidomethyl)furan-*2*-carboxylic acid (**3c**) were obtained in similar yield as during the enzyme screening with 54 % and 61 % respectively (Table 3, Figures S1-36-37). *5*-(octanamidomethyl)furan-*2*-carboxylic acid (**5c**) was however less produced with 26 % yield after 24 h (Table 3, Figure S1-S39). However, this result should be interpretated with caution, as the amide solubility was found to be low, potentially leading to an underestimation of its concentration by the ^{1}H NMR monitoring. Finally, succinic acid was also less converted than during the ACL screening, but 24 % of amide was formed (Table 3, Figure S38), including 2/3 of diamide derivative (*5*-((*4*-((*5*-carboxyfuran-*2*-yl)amino)-*4*-oxobutanamido)methyl)furan-*2*-carboxylic acid (**11d**))(Figure S1). This could be due to insufficient amine/carboxylic acid ratio, as succinic acid is a di-carboxylic acid. Despite this, it demonstrates the enzyme's ability to act on the mono-amide as a substrate (*5*-((*3*-carboxypropanamido)methyl)furan-*2*-carboxylic acid (**11c**)), with a good activity as the mono-amide didn't accumulate in the reaction mixture.

Table 4

Finally, we scaled-up the model reaction on butanol (**1a**), and we conducted the process at 20 mL scale. To reduce the carbon cost of the reaction, we decided to use only 1.1 AMFC equivalent, compared to the 5 equivalents used in small-scale reactions (Figure 3). We observed a slightly lower butanol conversion, with 86 % yield in butanoic acid in 24h. Not surprisingly with just 1.1 equivalent AMFC in the reaction media, only 36 % amide formation was achieved after 24 h in the 2nd step (Table 4). While this result may seem modest, it is very promising. There are several possibilities for improvement, while maintaining a low carbon cost, such as implementing an ATP regeneration system, as recently highlighted by the authors of this article.[13]

Experimental

Chemicals

All reagents were purchased from commercial sources and used without additional purification. AMFC hydrochloride form was used for all reactions. Pyruvate Kinase, from rabbit muscle (PK, P9136), L-Lactic Dehydrogenase, from rabbit muscle (LDH, L1254), Myokinase, from rabbit muscle (MK, M3003), Phospho(enol)pyruvic acid monopotassium salt (PEP-K, 860077), β-Nicotinamide adenine dinucleotide, reduced dipotassium salt (NADH, N4505) were purchased from Sigma Aldrich.

HPLC-RI

Analyses were performed using HPLC Shimadzu coupled with RI detector and equipped with Aminex HPX-87H (BIO-RAD column) (300 x 7.8 mm; 9 µm).
Conditions: mobile phase was H_2SO_4 (5 mM) eluted with a flow rate of 0.7 mL.min^{-1} for 60 min (Isocratic) at 60 °C. Injection volumes of 10 µL were used for all samples.

^{1}H NMR measurements

The ^{1}H spectra were recorded at room temperature on a Bruker Advance 300 spectrometer (Bruker, USA). Coupling constants were measured in Hertz (Hz) and multiplicities for ^{1}H NMR coupling were presented as s (singlet), d (doublet), t (triplet), q (quintuplet), h (hexuplet) and m (multiplet). Chemical shifts are reported relative to the sodium trimethylsilylpropionate reference.

Catalyst synthesis

To 200 mL of distilled water under vigorous stirring were added dropwise 115 mg of a 30 % (w/w) solution of the metal precursor ($HAuCl_4$) followed by 1.2 mL of a 2 % polyvinylalcohol water solution. Then, 5 mL of a 0.2 M $NaBH_4$ water solution was added dropwise, and the reaction mixture was stirred for 30 min, then 1 g of CaO was added. The amount of support was calculated to give a total final metal loading of 2 wt.% (nominal). The solution was kept under stirring for 2 h. Afterwards, the solid was filtrated, washed with hot distilled water (2 x 25 mL) and ethanol (2 x 25 mL), and then dried at 100 °C for 1 h. The metal loading was determined using ICP analysis.

Protein expression and purification

All steps from primers purchase to cell lysate preparation were carried out as previously described.[38] The enzyme was purified by loading the cell-free extract onto a Ni-NTA column (QIAGEN) according to the manufacturer's instructions. The elution buffer was 50 mM sodium potassium phosphate (pH 7.5), 50 mM NaCl, 250 mM imidazole and 10 % glycerol and the desalting buffer was 50 mM phosphate (pH 7.5), 50 mM NaCl and 10 % glycerol. Large-scale purification was conducted from a 500 mL culture by nickel affinity chromatography in tandem with desalting (HiPrep 26/10 17-5087-01) as described elsewhere.[39] Protein concentration was determined by the Bradford method with bovine serum albumin as the standard. The samples were analyzed by SDS-PAGEs using the Invitrogen NuPage system. The purified proteins were stored at -80 °C.

ACL screening

All the reactions were conducted from triplicate in a final reaction volume of 50 µL. To a reaction mixture containing carboxylic acid (5 mM), AMFC (25 mM), ATP (5 mM), $MnCl_2$ (5 mM) and $MgCl_2$ (5 mM) in MOPS buffer (50 mM; pH 8) with 2.5 % DMSO for all substrates except compounds **5**, **6** and **9**: 5 % DMSO (v/v) was added 0.1 mg.mL^{-1} of purified enzyme. The reactions, in 96-microwell plates, were stirred at 130 rpm in a Cole-Parmer™ shaker incubator at 60 °C for 24 h. Negative control reactions in absence of enzyme or substrate were performed in parallel.

Enzymatic screening assay

Enzymatic spectrophotometric assays were performed in microplates on a SpectraMax Plus384 (Molecular Devices, Sunnyvale, USA. Amide formation was monitored by coupled enzymatic assay. AMP release resulting from amide formation, is coupled to the consumption of NADH by three enzymatic steps allowing spectrophotometric monitoring at 340 nm (Scheme S1).
The enzymatic assay mixture consists of 50 mM glycine-glycine buffer pH 7.5, 2.5 mM PEP-K, 0.5 mM ATP, 1 mM $MgCl_2$, 1 mM $MnCl_2$, 1.7 mM NADH, 1 U PK, 2.3 U LDH. To 70 µl of the assay mixture, 10 µl of the ACL reaction sample were added for an initial optical density measurement. Then, 20 µl of 1 U MK were added to initiate the reaction. All reactions were conducted at 25 °C in 96-microwell plates. Absorbance at 340 nm was measured immediately and monitored for 15 min. Calibration curves, as well as controls without substrate or without enzyme, were established in the same manner in duplicates. Conversion was determined by measuring the optical density difference resulting from AMP release. The limit of quantification was estimated at 4.5% conversion; results below this threshold are not reported.

Buffer screening with oxidation catalyst

4 mg of Au/CaO were added to 1 mL of stock solution containing alcohol (5 mM) in 50 mM buffer (MOPS, pH 8-9; TRIS-HCl pH 9-10; CAPS pH 10-11) supplemented with $MgCl_2$ (5 mM) or $MnCl_2$ (5 mM), or a mix of two (5 mM each), in a sealed GC vial. The vials were rotated on a rotary shaker (revolving tube, thermoscientific, USA) at 25 rpm at 60 °C for 24 h. Reaction was monitored by HPLC-RI (Figure S6-17).

Alcohols oxidation screening

4 mg of Au/CaO were added to 1 mL of stock solution containing alcohol (5 mM) in MOPS buffer (50 mM; pH 8) supplemented with $MgCl_2$ (5 mM) in a sealed GC vial. The vials were rotated on a rotary shaker (revolving tube, thermoscientific, USA) at 25 rpm at 60 °C for 24 h. Reaction was monitored ^{1}H NMR for butanol (**1a**), pentanol (**2a**), hexanol (**3a**), octanol (**5a**), *2*-phenylethanol (**7a**) and *1,4*-butandiol (**11a**) (Table 2 and Figure S20-24).

Hybrid process

To 1 mL of a solution containing alcohol (10 mM) in MOPS buffer (50 mM; pH 8) supplemented with $MgCl_2$ (5 mM) were added 8 mg of Au/CaO. The reaction mixture was then placed on a rotary shaker (revolving tube, thermoscientific, USA) at 60 °C for 24 h. The carboxylic acid formation was monitored by ^{1}H NMR. Then, ACL was added to the reaction mixture at a final concentration of 0.15 mg.mL^{-1}, along with AMFC (25 mM final) and ATP (50 mM final), as well as $MgCl_2$ to maintain a final concentration of 5 mM. The final volume of reaction was of 2 mL. The solution placed at 60 °C for 24 h. Products formation was followed by ^{1}H NMR (Figures S25-39).

Hybrid process scale up

To 20 mL of a solution containing alcohol (10 mM) in MOPS buffer (50 mM; pH 8) supplemented with $MgCl_2$ (5 mM) were added 80 mg of Au/CaO. The reaction mixture was then placed on a rotary shaker (revolving tube, thermoscientific, USA) at 60 °C for 24 h. The carboxylic acid formation was monitored by ^{1}H NMR. Then, ACL was added to the reaction mixture at a final concentration of 0.15 mg.mL^{-1}, along with AMFC (5.5 mM final) and ATP (50 mM final), as well as $MgCl_2$ to maintain a final concentration of 5 mM. The final volume of reaction was of 2 mL. The solution placed at 60 °C for 24 h. Products formation was followed by ^{1}H NMR (Figures S44-55).

Characterization of *5*-(pentanamidomethyl)furan-*2*-carboxylic acid (2c)

To have a reference for analysis, *5*-(pentanamidomethyl)furan-*2*-carboxylic acid (**2c**) was synthesized by conventional organic chemistry (Figure S1). The reaction was performed in suspension, in anhydrous media. Sodium *5*-(pentanamidomethyl)furan-*2*-carboxylate was mixed with a large excess of pyridine before 1.5 eq. of pentanoyl chloride was slowly added at room temperature. While adding the chloride, an ice bath was used to maintain the temperature of the reaction media below 30 °C. The reaction was then vigorously stirred for 24 h at room temperature. Finally, the product was poured on HCl acidified ice to pH = 2 and extracted with dichloromethane.
^{1}H NMR (300 MHz, DMSO-D_6, 298 K): δ = 7.13 (d, J = 3.4 Hz, 1H, H_3), 6.37 (d, J = 3.5 Hz, 1H, H_4), 4.29 (d, J = 5.7 Hz, 2H, H_6), 2.12 (t, J = 7.4 Hz, 2H, H_8), 1.49 (q, J = 6 Hz, 2H, H_9), 1.26 (h, J = 9 Hz, 2H, H_{10}), 0.86 (t, J = 7.3 Hz, 3H, H_{11}). (Figure S40).
^{13}C NMR (75 MHz, DMSO-D_6, 298 K): δ = 172.74 (C1), 159.68 (C7), 157.52 (C2), 144.25 (C5), 119.17 (C3), 109.35 (C4), 36.11 (C6), 35.33 (C8), 27.80 (C9), 22.22 (C10), 14.15 (C11). (Figure S41).
HSQC available in Figure S43.

Conclusion

In conclusion, we have successfully constructed a tandem catalytic process for the functionalization of AMFC by synthesis of AMFC-derived amides from alcohols *via* combination of gold-catalyzed oxidation reaction with acyl-CoA ligase-promoted amidation. These results illustrate the potential of biosourced AMFC as a platform molecule. The Au/CaO chemical catalyst achieved complete conversion of all tested aliphatic mono- and di-alcohols, ranging from C4 to C8, using atmospheric dioxygen as the sole oxidant. Moreover, this heterogeneous catalytic step was conducted under conditions compatible with subsequent enzymatic use, offering significant atom economy and reducing the process's associated hazards. In parallel, eight acyl-CoA ligases were screened against 12 mono- and di- carboxylic acid substrates. Overall, all the enzymes showed good activity and enabled the conversion of a broad range of carboxylic acids. One enzyme, *Ts*ACL, was revealed to be highly promiscuous and was retained for developing the tandem catalytic process. The hybrid process, which sequentially combines these two catalysts in a single pot was devised to yield the corresponding amide derivatives. Using AMFC as the nucleophilic amine, this

one pot-two steps process achieved yields of up to 64 % in 24 h. One limitation of this process is the use of large excess of ATP, but this could be easily circumvented by setting up an ATP regeneration system.[13] Another avenue for improvement is to implement a fully integrated process in a single step, ideally using catalyst compartmentalization techniques to obtain a multi-catalytic hybrid materials.[2] This tandem heterogeneous enzymatic catalysis, performed under mild aqueous conditions, marks a significant advancement through the integration of gold nanoparticles and enzyme within a single reaction vessel. This innovative approach provides a groundbreaking method for the functionalization of the biosourced AMFC platform molecule.

Author contributions

AZ and EH conceived the project. AZ, EH, JB, AL, AFJ, LB, RM, MB and CVV designed and conducted the experiments, with input of LM, VH, and RF. LB, RM, AFJ, JB, AL, CVV, AZ and EH analyzed data with input from LM, VH and RF. EH and AZ wrote the manuscript with input from LB, RM, AFJ, JB, AL, FM, CVV, LM, VH, MB and RF.

Conflicts of interest

There are no conflicts to declare

Data availability

All chromatograms (including calibration curves) and NMR spectra produced in this study are listed in the Supporting Information.

Acknowledgements

Part of this work was performed using equipment of the REALCAT platform, funded by a French governmental subsidy managed by the French National Research Agency (ANR) within the framework of the "Future Investments' program (ANR-11-EQPX-0037). The Hauts-de-France region, FEDER, Ecole Centrale de Lille, and Centrale Initiatives Foundation are also warmly acknowledged for their financial contributions to the acquisition of the REALCAT platform equipment. This research was funded, in whole or in part, by the I-Site ULNE. A CC-BY public copyright license has been applied by the authors to the present document and will be applied to all subsequent versions up to the Author Accepted Manuscript arising from this submission, in accordance with the grant's open access conditions.

Notes and references

1 H. C. Erythropel, J. B. Zimmerman, T. M. de Winter, L. Petitjean, F. Melnikov, C. H. Lam, A. W. Lounsbury, K. E. Mellor, N. Z. Janković, Q. Tu, L. N. Pincus, M. M. Falinski, W. Shi, P. Coish, D. L. Plata and P. T. Anastas, *Green Chem.*, 2018, **20**, 1929–1961.
2 E. Heuson, R. Froidevaux, I. Itabaiana, R. Wojcieszak, M. Capron and F. Dumeignil, *Green Chem.*, 2021, **23**, 1942–1954.
3 D. P. Debecker, V. Smeets, M. Van der Verren, H. Meersseman Arango, M. Kinnaer and F. Devred, *Curr. Opin. Green Sustain. Chem.*, 2021, **28**, 100437.
4 E. Heuson and F. Dumeignil, *Catal. Sci. Technol.*, 2020, **10**, 7082–7100.
5 J. Pitzer and K. Steiner, *J. Biotechnol.*, 2016, **235**, 32–46.
6 Y. Jiang and K. Loos, *Polymers*, 2016, **8**, 243.
7 Q.-M. Gu, W. W. Maslanka and H. N. Cheng, in *Polymer Biocatalysis and Biomaterials II*, American Chemical Society, 2008, vol. 999, pp. 309–319.
8 D. J. C. Constable, P. J. Dunn, J. D. Hayler, G. R. Humphrey, J. Johnnie L. Leazer, R. J. Linderman, K. Lorenz, J. Manley, B. A. Pearlman, A. Wells, A. Zaks and T. Y. Zhang, *Green Chem.*, 2007, **9**, 411–420.
9 R. M. Lanigan and T. D. Sheppard, *Eur. J. Org. Chem.*, 2013, **2013**, 7453–7465.
10 V. R. Pattabiraman and J. W. Bode, *Nature*, 2011, **480**, 471–479.
11 B. M. Dorr and D. E. Fuerst, *Curr. Opin. Chem. Biol.*, 2018, **43**, 127–133.
12 T. Abe, Y. Hashimoto, S. Sugimoto, K. Kobayashi, T. Kumano and M. Kobayashi, *J. Antibiot. (Tokyo)*, 2017, **70**, 435–442.
13 C. M. Lelièvre, M. Balandras, J.-L. Petit, C. Vergne-Vaxelaire and A. Zaparucha, *ChemCatChem*, 2020, **12**, 1184–1189.
14 P. M. Marchetti, S. M. Richardson, N. M. Kariem and D. J. Campopiano, *MedChemComm*, 2019, **10**, 1192–1196.
15 M. Petchey, A. Cuetos, B. Rowlinson, S. Dannevald, A. Frese, P. W. Sutton, S. Lovelock, R. C. Lloyd, I. J. S. Fairlamb and G. Grogan, *Angew. Chem. Int. Ed.*, 2018, **57**, 11584–11588.
16 M. R. Petchey and G. Grogan, *Adv. Synth. Catal.*, 2019, **361**, 3895–3914.
17 S. Sarak, S. Sung, H. Jeon, M. D. Patil, T. P. Khobragade, A. D. Pagar, P. E. Dawson and H. Yun, *Angew. Chem. Int. Ed.*, 2021, **60**, 3481–3486.
18 A. J. L. Wood, N. J. Weise, J. D. Frampton, M. S. Dunstan, M. A. Hollas, S. R. Derrington, R. C. Lloyd, D. Quaglia, F. Parmeggiani, D. Leys, N. J. Turner and S. L. Flitsch, *Angew. Chem.*, 2017, **129**, 14690–14693.
19 M. Zhu, L. Wang and J. He, *ACS Chem. Biol.*, 2019, **14**, 256–265.
20 N. Capra, C. Lelièvre, O. Touré, A. Fossey-Jouenne, C. Vergne-Vaxelaire, D. B. Janssen, A.-M. W. H. Thunnissen and A. Zaparucha, *Front. Catal.*, , DOI:10.3389/fctls.2024.1360129.
21 H. K. Philpott, P. J. Thomas, D. Tew, D. E. Fuerst and S. L. Lovelock, *Green Chem.*, 2018, **20**, 3426–3431.
22 T. Abe, Y. Hashimoto, H. Hosaka, K. Tomita-Yokotani and M. Kobayashi, *J. Biol. Chem.*, 2008, **283**, 11312–11321.
23 J. Zhang, E. Kao, G. Wang, E. E. K. Baidoo, M. Chen and Jay. D. Keasling, *Metab. Eng. Commun.*, 2016, **3**, 1–7.
24 T. Mori, K. Wanibuchi, H. Morita and I. Abe, *Chem. Pharm. Bull. (Tokyo)*, 2021, **69**, 717–720.
25 S. ; G.-F. González-Granda V., in *Dynamic Kinetic Resolution (DKR) and Dynamic Kinetic Asymmetric Transformations (DYKAT)*, Georg Thieme Verlag KG, Stuttgart, 1st edition., 2022, vol. 2022/4.
26 S. González-Granda, L. Escot, I. Lavandera and V. Gotor-Fernández, *Angew. Chem.*, 2023, **135**, e202217713.
27 H. Gröger, F. Gallou and B. H. Lipshutz, *Chem. Rev.*, 2023, **123**, 5262–5296.
28 L. Bering, J. Thompson and J. Micklefield, *Trends Chem.*, 2022, **4**, 392–408.
29 S. González-Granda, L. Escot, I. Lavandera and V. Gotor-Fernández, *ACS Catal.*, 2022, **12**, 2552–2560.
30 C. Gastaldi, G. Mekhloufi, C. Forano, A. Gautier and C. Guérard-Hélaine, *Green Chem.*, 2022, **24**, 3634–3639.
31 L. Escot, S. González-Granda, V. Gotor-Fernández and I. Lavandera, *Org. Biomol. Chem.*, 2022, **20**, 9650–9658.
32 S. González-Granda, I. Lavandera and V. Gotor-Fernández,

Angew. Chem., 2021, **133**, 14064–14070.
33 Q. Wang, X. Zhang, L. Huang, Z. Zhang and S. Dong, *Angew. Chem. Int. Ed.*, 2017, **56**, 16082–16085.
34 A. Lancien, R. Wojcieszak, E. Cuvelier, M. Duban, P. Dhulster, S. Paul, F. Dumeignil, R. Froidevaux and E. Heuson, *ChemCatChem*, 2021, **13**, 247–259.
35 T. K. Chakraborty, S. Tapadar and S. Kiran Kumar, *Tetrahedron Lett.*, 2002, **43**, 1317–1320.
36 N. Perchat, P.-L. Saaidi, E. Darii, C. Pellé, J.-L. Petit, M. Besnard-Gonnet, V. de Berardinis, M. Dupont, A. Gimbernat, M. Salanoubat, C. Fischer and A. Perret, *Proc. Natl. Acad. Sci. U. S. A.*, 2018, **115**, E4358–E4367.
37 A. S. Hawkins, Y. Han, R. K. Bennett, M. W. W. Adams and R. M. Kelly, *J. Biol. Chem.*, 2013, **288**, 4012–4022.
38 C. Vergne-Vaxelaire, F. Bordier, A. Fossey, M. Besnard-Gonnet, A. Debard, A. Mariage, V. Pellouin, A. Perret, J.-L. Petit, M. Stam, M. Salanoubat, J. Weissenbach, V. De Berardinis and A. Zaparucha, *Adv. Synth. Catal.*, 2013, **355**, 1763–1779.
39 N. Perchat, P.-L. Saaidi, E. Darii, C. Pellé, J.-L. Petit, M. Besnard-Gonnet, V. de Berardinis, M. Dupont, A. Gimbernat, M. Salanoubat, C. Fischer and A. Perret, *Proc. Natl. Acad. Sci.*, 2018, **115**, E4358–E4367.

Figures

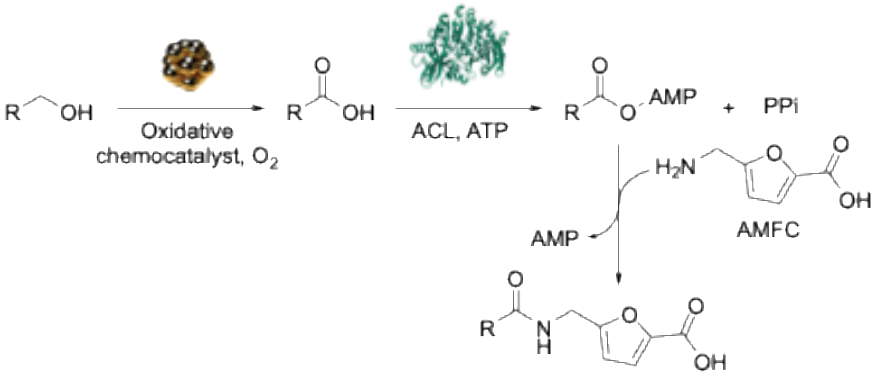

Scheme 1: General scheme for the synthesis of AMFC-based amides through the implementation of a one-pot/two-steps process combining supported gold nanoparticles as oxidative chemocatalyst and a CoA ligase (ACL) as biocatalyst.

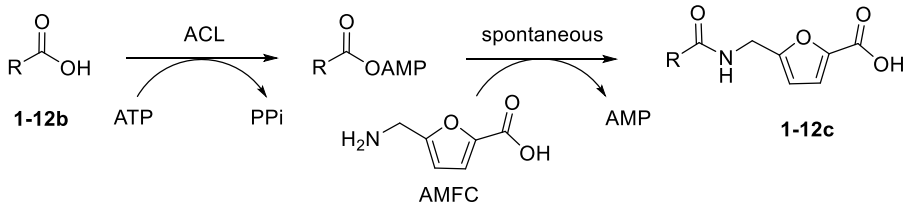

Scheme 2: Amide formation by chemoenzymatic two-step reaction catalyzed by ACL.

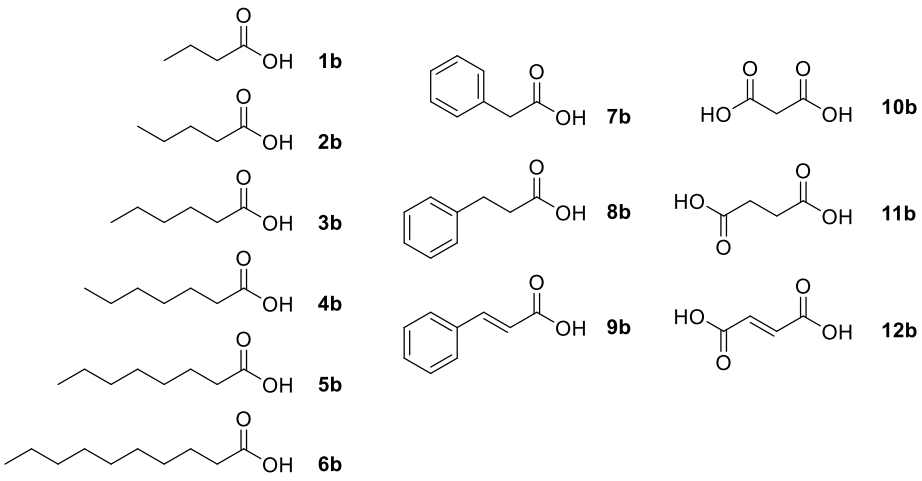

Figure 1: Structures of mono and di carboxylic acid substrates for ACL screening.

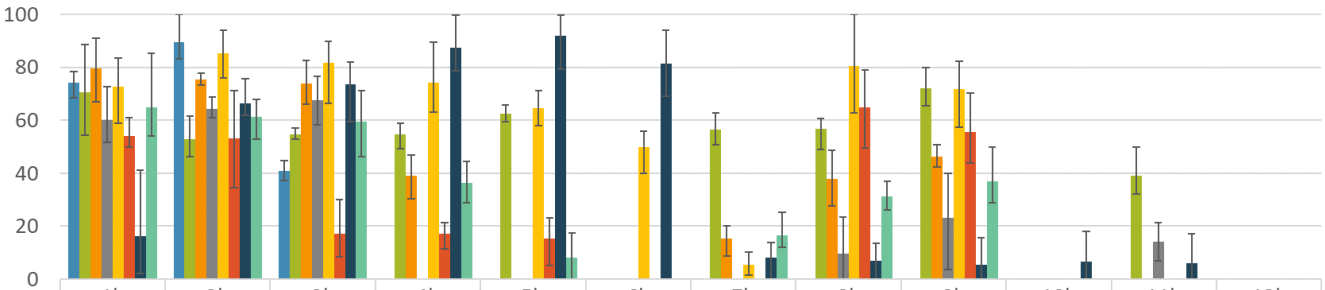

	1b	2b	3b	4b	5b	6b	7b	8b	9b	10b	11b	12b
MsACL	74	90	41	0	0	0	0	0	0	0	0	0
TsACL	71	53	55	55	63	0	56	57	72	0	39	0
GtACL	80	75	74	39	0	0	15	38	46	0	0	0
MsACL2	60	64	68	0	0	0	0	10	23	0	14	0
GtACL2	73	85	82	74	65	50	5	81	72	0	0	0
TtACL	54	53	17	17	15	0	0	65	55	0	0	0
ChACL	16	67	74	88	92	82	8	7	5	7	6	0
StACL	65	61	59	36	8	0	17	31	37	0	0	0

Figure 2: Analytical yields of AMFC-derived amides from carboxylic acids catalyzed by ACLs. Reaction conditions: carboxylic acid (5 mM), AMFC (25 mM), ATP (5 mM), $MnCl_2$ (5 mM), $MgCl_2$ (5 mM), MOPS buffer (50 mM; pH 8) with 2.5 % DMSO for all substrates except compounds **5b**, **6b** and **9b**: 5 % DMSO (v/v), 0.1 mg.mL^{-1} of purified enzyme, 130 rpm at 60 °C for 24 h. Analytical yields were deduced from calibration curves by spectrophotometric assay (Figure S2). The uncertainties are those generated by the fitting of data averaged over three experiments.

Table 1: Analytical yield of butanol oxidation by Au/CaO at 60 °C after 24 h in MOPS, TRIS-HCl and CAPS buffer, with pH ranging from 8 to 11, in presence of $MgCl_2$, $MnCl_2$ or $MgCl_2$ + $MnCl_2$

Buffer	Metal ion	Butyric acid yield
MOPS pH 8	5 mM $MgCl_2$	79 %
MOPS pH 9	5 mM $MgCl_2$	84 %
TRIS-HCl pH 9	5 mM $MgCl_2$	0 %
TRIS-HCl pH 10	5 mM $MgCl_2$	0 %
CAPS pH 10	5 mM $MgCl_2$	36 %
CAPS pH 11	5 mM $MgCl_2$	56 %
MOPS pH 8	5 mM $MnCl_2$	48 %
MOPS pH 8	5 mM $MgCl_2$ + 5 mM $MnCl_2$	50 %

Table 2: Analytical yield of acid formation catalyzed by Au/CaO catalyst in MOPS pH 8 in 24 h at 60 °C in presence of 5 mM $MgCl_2$

Substrate	Acid yield[a]
Butanol (**1a**)	94 % in **1b**
Pentanol (**2a**)	91 % in **2b**
Hexanol (**3a**)	93 % in **3b**
Octanol (**5a**)	88 % in **5b**
1,2-Butanediol (**11a**)	> 95 % in **11b**

[a] yield determined by ^{1}H NMR analysis

Table 3: Analytical yields of acid and amide after the first and second steps (24 h each) of the one-pot/two-steps process

Substrate	Acid yield after 24 h[a]	Amide yield after 24 h[a]
Butanol (**1a**)	94 % in **1b**	65 % in **1c**
Pentanol (**2a**)	90 % in **2b**	54 % in **2c**
Hexanol (**3a**)	91 % in **3b**	61 % in **3c**
Octanol (**5a**)	88 % in **5b**	26 % in **5c**
1,2-Butanediol (**11a**)	> 95 % in **11b**	8 % in **11c** and 16 % in **11d**

[a] yield determined by ^{1}H NMR analysis

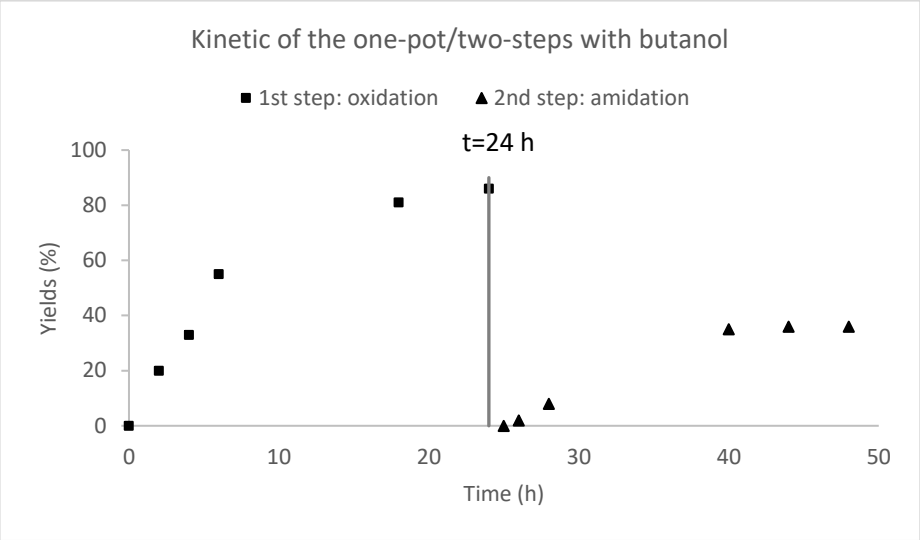

Figure 4: Kinetic of the one-pot/two-steps process with butanol as starting alcohol. The vertical bar corresponds to the AMFC addition time point, along with enzyme and ATP. The left-hand side of the graph shows the evolution of butanoic acid yield. The right-hand side of the graph shows the evolution of 5-(butyramidomethyl)furan-2-carboxylic acid yield.

Table 4: Analytical yield over time of the one-pot/two-steps reaction in larger scale (20 mL)

	Reaction time	Butanol (**1a**)[a,b]	Butanoic acid (**1b**)[a,b]	Amide (**1c**)[a,c]
1st Step: oxidation by Au/CaO	0 h	100 %	0 %	---
	2 h	80 %	20 %	---
	4 h	67 %	33 %	---
	6 h	45 %	55 %	---
	18 h	19 %	81 %	---
	24 h	14 %	86 %	---
2nd Step: amidation by ACL	25 h	---	---	0 %
	26 h	---	---	2 %
	28 h	---	---	8 %
	40 h	---	---	35 %
	44 h	---	---	36 %
	48 h	---	---	36 %
Enzyme addition	60 h	---	---	36 %
$MgCl_2$ addition	231 h	---	---	50 %

[a] yield measured from ^{1}H NMR analysis

[b] yield calculated using the acid/alcohol ratio (based on the 2.09 ppm triplet for butanoic acid (**1b**), and 3.54 ppm triplet for butanol (**1a**))

[c] yield calculated using the amide (**1c**)/AMFC ratio (based on the 6.29 ppm doublet for the amide (**1c**), and 6.84 ppm doublet for AMFC)